

VOLUME 115, NUMBER 1  
JANUARY 13, 1993  
© Copyright 1993 by the  
American Chemical Society

---

# JOURNAL OF THE AMERICAN CHEMICAL SOCIETY

---

## *EDITORIALS*

---

### **New Page Limit for Communications**

The American Chemical Society will soon begin using a new composition system for the *Journal of the American Chemical Society* in which all Articles and Communications will begin at the top of a page. Therefore, the length of Communications in the *Journal* will be extended. In the future, Communications will be strictly limited to two journal pages or roughly the equivalent of 1500 words plus references. Guidelines for estimating the length of Communications are given in the Notice to Authors of Papers, which is published in the first issue of each volume of the *Journal*. However, the total space required for a Communication may be difficult to estimate exactly and will depend upon the number of figures, schemes, tables, and references, and the Journals Department has been authorized to require authors, without exception, to shorten their Communications when they exceed the two-page limit. This mandatory shortening will take place in the page-proof stage of production.

### **Availability of Supplementary Material via Internet**

Starting in 1993, supplementary material will be available electronically through the Internet, direct modem access, and via FAX delivery. This material will also continue to be available on microfiche, microfilm, and photocopy. Authors are encouraged to submit supplementary material as ASCII files, in addition to the traditional hard copies, to make the supplementary data more useful. Details about the costs and accessing this material electronically are given on the current *Journal of the American Chemical Society* masthead page.

## Articles

### New Insights into the Enzymatic Catalysis of the Oxidation of Glucose by Native and Recombinant Glucose Oxidase Mediated by Electrochemically Generated One-Electron Redox Cosubstrates

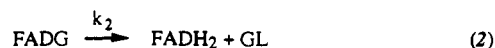
Christian Bourdillon,<sup>1a</sup> Christophe Demaille,<sup>1b</sup> Jacques Moiroux,<sup>\*.1b</sup> and Jean-Michel Savéant<sup>\*.1b</sup>

Contribution from the Laboratoire de Technologie Enzymatique, Unité Associée au CNRS No. 1442, Université de Technologie de Compiègne, B.P. 649, 60206 Compiègne, Cedex, France, and the Laboratoire d'Electrochimie Moléculaire de l'Université Denis Diderot (Paris 7), Unité Associée au CNRS No. 438, 2 place Jussieu 75251 Paris Cedex 05, France.  
Received July 24, 1992

**Abstract:** Cyclic voltammetry may be efficiently used to investigate the catalysis of glucose oxidation by glucose oxidase using one-electron redox mediators. Provided that sufficient deviation from the first-order kinetics is created and duly analyzed, it allows for the simultaneous determination of the rate constants of both the reductive half-reaction and the oxidation of the reduced enzyme by the one-electron redox mediator. Controlled achievement of the first-order conditions leads to the exact determination of the oxidation rate constant, thus allowing for the detection of significant variations with pH in contrast with its reputed insensitivity to this parameter. These variations involve as characteristic  $pK_s$  those of the  $FADH_2/FADH^-$  and  $FADH^+/FAD^{2+}$  couples and may be rationalized by a kinetic scheme in which the various protonated forms of the flavins at the three successive oxidation states are taken into account. Analysis of the catalytic response as a function of the pH and the driving forces offered by the various one-electron mediators points to the formation of a precursor complex between the mediator and the enzyme. Enzyme differentiation between the various one-electron mediators then derives from the variations of the thermodynamics and kinetics of the precursor complex formation.

Flavoprotein glucose oxidase ( $\beta$ -D-glucose:oxygen 1-oxidoreductase, EC 1.1.3.4.) is certainly one of the most widely used enzymes in the field of enzyme technology. The fungal enzyme, usually extracted from *Aspergillus niger*, is a dimer of ca. 160 000 molecular weight, containing two identical and noninteracting flavin groups.<sup>2</sup> The gene for *A. niger* glucose oxidase has been isolated and cloned, and the primary structure of the protein was established recently.<sup>3</sup> The three-dimensional structure is not known at the moment, although the recent successful growths of crystals of an enzymatically deglycosylated glucose oxidase amenable to X-ray diffraction analysis<sup>4</sup> points to an impending elucidation.

The mechanism of the enzyme catalysis of the oxidation of  $\beta$ -D-glucose to glucono- $\delta$ -lactone and the concomitant reduction of the natural cosubstrate, i.e., molecular oxygen to hydrogen peroxide, has been investigated by means of spectrometric stop-flow techniques.<sup>5,6</sup> At this occasion, the kinetic characteristics of the "reductive half-reaction"



(FAD,  $FADH_2$  = oxidized and reduced forms of the prosthetic groups of glucose oxidase, respectively; G =  $\beta$ -D-glucose; GL = glucono- $\delta$ -lactone) have been determined.

The principle of the enzymatic catalysis of the electrochemical oxidation of glucose mediated by redox cosubstrates is sketched in Scheme I, where P and Q are the reduced and oxidized forms of the mediator (cosubstrate), respectively. Two types of artificial redox cosubstrates have been used as mediators:  $2e^- + H^+$  couples, such as the quinone/hydroquinone couple,<sup>7</sup> and one-electron redox couples. In the latter case, substituted ferrocenes have exclusively been employed either under the form of water-soluble derivatives<sup>8</sup> or grafted to the electrode inside a polymer matrix.<sup>9</sup>

Kinetic measurements using electrochemical techniques are based on the determination of the catalytic currents obtained in the presence of the mediator, the enzyme, and glucose. One starts with the reduced form of the mediator P and produces its oxidized form Q by appropriate poisoning or scanning of the electrode potential. For the method to be valid, the introduction of the enzyme should not affect the stability of Q. Introduction of glucose then

(1) (a) Université Technologique de Compiègne. (b) Université Denis Diderot.

(2) Pazur, J. H.; Kleppe, K. *Biochemistry* 1964, 3, 578.

(3) Frederick, K. R.; Tung, J.; Emerick, R. S.; Masiarz, F. R.; Chamberlain, S. H.; Vasavada, A.; Rosenberg, S.; Chakraborty, S.; Schopfer, L. M.; Massey, V. *J. Biol. Chem.* 1990, 265, 3793.

(4) (a) Kalisz, H. M.; Hecht, H. J.; Schomburg, D.; Schmid, R. D. *J. Mol. Biol.* 1990, 213, 207. (b) Hendle, J.; Hecht, H. J.; Kalisz, H. M.; Schmid, R. D.; Schomburg, D. *J. Mol. Biol.* 1992, 223, 1167. (c) Kalisz, H. M.; Hecht, H. J.; Schomburg, D.; Schmid, R. D. *Biochim. Biophys. Acta* 1991, 1080, 138.

(5) (a) Weibel, M. K.; Bright, H. J. *J. Biol. Chem.* 1971, 246, 2734. (b) Bright, H. J.; Appleby, M. *J. Biol. Chem.* 1969, 244, 3625.

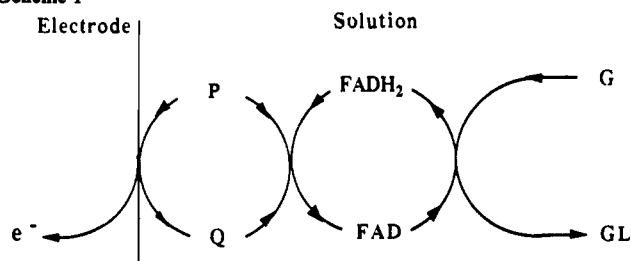
(6) Gibson, Q. H.; Swoboda, B. E. P.; Massey, V. *J. Biol. Chem.* 1964, 239, 3927.

(7) (a) Bourdillon, C.; Thomas, V.; Thomas, D. *Enzyme Microb. Technol.* 1982, 4, 175. (b) Bourdillon, C.; Hervagault, C.; Thomas, D. *Biotech. Bioeng.* 1985, 27, 1619. (c) Bourdillon, C.; Laval, J. M.; Thomas, D. *J. Electrochem. Soc.* 1986, 133, 706.

(8) (a) Cass, A. E. G.; Davis, G.; Francis, G. D.; Hill, H. A. O.; Aston, W. J.; Higgins, I. J.; Plotkin, E. V.; Scott, L. D. L.; Turner, A. P. F. *Anal. Chem.* 1984, 56, 667. (b) Green, M. J.; Hill, H. A. O. *J. Chem. Soc., Faraday Trans. 1* 1986, 82, 1237. (c) Liaudet, E.; Battaglini, F.; Calvo, E. J. *J. Electroanal. Chem.* 1990, 293, 55. (d) Rusling, J. F.; Ito, K. *Anal. Chim. Acta* 1991, 252, 23. (e) Frede, M.; Steckhan, E. *Tetrahedron Lett.* 1991, 32, 5063.

(9) (a) Heller, A. *Acc. Chem. Res.* 1990, 23, 128. (b) Schumann, W.; Ohara, T. J.; Schmidt, H. L.; Heller, A. *J. Am. Chem. Soc.* 1991, 113, 1394. (c) Heller, A. *J. Phys. Chem.* 1992, 96, 3579.

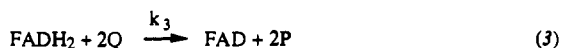
Scheme I



triggers an increase of the anodic current caused by the regeneration of P through the catalytic cycle depicted in Scheme I. This increase of the current potentially contains information concerning the kinetics of the catalytic reaction.

With quinone mediators,<sup>7</sup> a steady-state electrochemical technique was employed that consisted of setting the potential, in the presence of the hydroquinone and the enzyme, at a sufficiently positive value for the hydroquinone to be entirely converted into the quinone at the electrode surface. The addition of glucose then triggers a jump of the steady-state current caused by the catalytic reaction. It was possible with this technique to determine the kinetics of the reductive half-reaction as evoked earlier, leading to values in agreement with previous values derived from stop-flow experiments in which dioxygen was used as the cosubstrate.

A transient electrochemical technique, cyclic voltammetry, was used in the studies in which substituted ferrocenes were employed as mediators.<sup>8</sup> Since the glucose/gluconolactone and FADH<sub>2</sub>/FAD couples are 2e<sup>-</sup> + 2H<sup>+</sup> systems, 2 equiv of ferrocene and ferrocenium are involved in the mediation. This can therefore be represented globally by



Possible mechanisms for reaction 3 will be discussed later. Thus, eq 1 (assuming that the steady-state approximation applies to FAD,

$$\frac{\partial[\text{Q}]}{\partial t} = D \frac{\partial^2[\text{Q}]}{\partial x^2} - \frac{2k_3 C_E^0 [\text{Q}]}{1 + k_3 \left( \frac{1}{k_2} + \frac{k_{-1} + k_2}{k_1 k_2 [\text{G}]} \right) [\text{Q}]} \quad (1)$$

FADG, and FADH<sub>2</sub>) governs the time and space distribution of the oxidized form of the mediator (in the framework of linear diffusion). (For eq 1, *t* = time; *x* = distance from the electrode; *D* = diffusion coefficient of Q; C<sub>E</sub><sup>0</sup> = total concentration of enzyme.)

Previous studies involving ferrocenes as mediators<sup>8</sup> have, unfortunately, considered only the limiting "pseudo-first-order" case, i.e.

$$\frac{\partial[\text{Q}]}{\partial t} = D \frac{\partial^2[\text{Q}]}{\partial x^2} - 2k_3 C_E^0 [\text{Q}]$$

thought to be applicable because large concentrations of glucose were used. This strategy has the advantage of simplifying the extraction of the kinetic information from the cyclic voltammetric data but suffers from two serious drawbacks. One is that, as can be seen from eq 1, a large concentration of glucose is not a sufficient condition for the pseudo-first-order approximation to be valid since, in addition,  $k_3[\text{Q}]/k_2$  should be negligible, vis à vis 1. The neglect of this additional condition may therefore lead to erroneous rate data. The other is that such a strategy impedes the determination of the kinetic parameters of the reductive half-reaction (reactions 1 and 2).

We will show in the following section that analysis of the cyclic voltammetric data by means of the full eq 1 is a perfectly workable task, allowing the simultaneous determination of the rate parameters of the reductive half-reaction and of the overall rate constant *k*<sub>3</sub> under various experimental conditions. *k*<sub>3</sub> is indeed a global rate constant, resulting from a series of elementary steps in which each of the two electrons and two protons involved in reaction 3 is exchanged. In this connection, it is surprising that

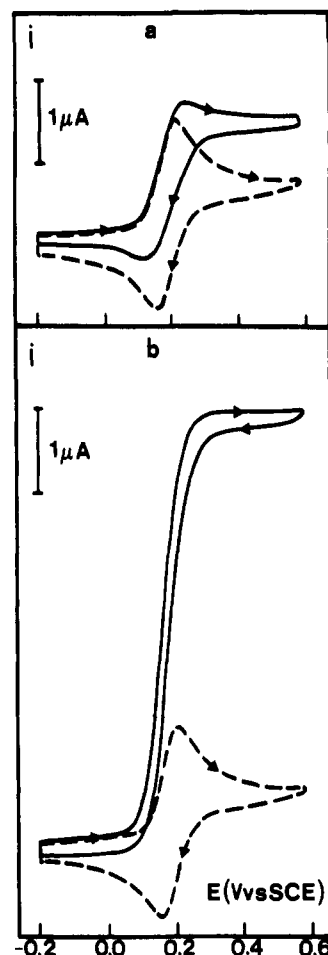
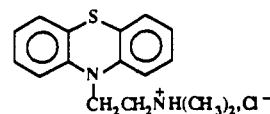


Figure 1. Glucose oxidase catalyzed electrochemical oxidation of  $\beta$ -D-glucose mediated by ferrocenemethanol. Dashed lines are cyclic voltammograms of ferrocenemethanol (0.1 mM) in the absence or presence of glucose (0.5 M). Full lines are voltammograms obtained upon addition of glucose oxidase (2.7  $\mu\text{M}$ ). Scan rate = 0.08 V s<sup>-1</sup>; temperature = 25 °C; ionic strength = 0.1 M. (a) acetate buffer, pH = 4.5. (b) phosphate buffer, pH = 6.5.

no pH dependence of the global rate constant *k*<sub>3</sub> has been so far detected.<sup>8a-c,10</sup> We have investigated systematically this problem by using a series of differently substituted ferrocenium mediators of different standard potentials and global charges, and we did find a clear indication of such a pH dependence. In the interpretation of the pH-dependent rate data, we have made use of thermodynamic data, standard potentials, and p*K*<sub>a</sub>s that have been previously gathered in the case of free<sup>11</sup> and enzyme-bound flavins.<sup>12</sup>

The rate data that we have gathered with a series of differently substituted ferroceniums as well as with another one-electron mediator from a different family, the promazine cation



(10) (a) A notable exception is the oxidation of the semiquinone form of FAD by a nitroxide radical (4-hydro-2,2,6,6-tetramethylpiperidine-1-oxyl), the rate constant of which has been found to decrease upon raising the pH with a midpoint located at 7.2.<sup>10b</sup> It should be noted, however, that the oxidizing system is a 1e<sup>-</sup> + H<sup>+</sup> couple in this case, unlike ferroceniums that may accept one electron but no proton. (b) Chan, T. W.; Bruice, T. C. *J. Am. Chem. Soc.* 1977, 99, 2387.

(11) (a) Williams, R. F.; Bruice, T. C. *J. Am. Chem. Soc.* 1976, 98, 7752. (b) Williams, R. F.; Shinkai, S. S.; Bruice, T. C. *J. Am. Chem. Soc.* 1977, 99, 921. (c) Eberlein, G.; Bruice, T. C. *J. Am. Chem. Soc.* 1982, 104, 1449.

(12) (a) Stankovich, M. T.; Shopfer, L. M.; Massey, V. *J. Biol. Chem.* 1978, 253, 4971. (b) Ghisla, S.; Massey, V. *Eur. J. Biochem.* 1989, 181, 1.

will also serve as a base for a discussion of the factors that control the reactivity of the flavin site toward one-electron cosubstrates. Concerning the question of the steric accessibility of the flavin center, we have compared the kinetics observed with the native *A. niger* enzyme to that observed with a recombinant glucose oxidase in which the periphery of the enzyme has been extensively glycosylated through N-linkages (350 000–400 000 molecular weight).<sup>3,13</sup>

### Results

Figure 1 shows two typical examples of catalytic currents observed with one of the ferrocenes we have investigated (ferrocenemethanol,  $E^0 = 0.19$  V vs SCE) at two pHs where catalysis is weak (pH = 4.5) and strong (pH = 6.5), respectively. In the latter case, the voltammogram exhibits a characteristic polarogram-like shape and the reverse trace is almost superimposable on the forward trace. This behavior indicates that the rate-determining step of the overall catalytic process is fast as compared to diffusion and that the consumption of the substrate in the diffusion-reaction layer is negligible.<sup>14</sup> At pH = 4.5, the current still tends toward a plateau but, nevertheless, exhibits a peak at less positive potential. At the same time, the reverse trace is clearly different from the forward trace, indicating a partial chemical reversibility. This behavior indicates that the consumption of the substrate within the diffusion-reaction layer is still negligible but that the catalytic process and diffusion have commensurate rates.

Within the series of experiments we have carried out, the concentration of the mediator,  $C_p^0$ , was varied from  $2.5 \times 10^{-6}$  to  $10^{-4}$  M and the concentration of glucose,  $C_G^0$ , from  $5 \times 10^{-3}$  to 0.5 M, while the concentration of enzyme,  $C_E^0$ , was always below  $3 \times 10^{-6}$  M.  $C_E^0$  is the molarity of the catalytically active FAD. The ensuing values of the ratio  $C_G^0/C_p^0$  (50 at minimum) were thus sufficiently large to ensure that the consumption of glucose within the diffusion-reaction layer is negligible. The glucose concentration could thus be regarded as constant and equal to the bulk concentration. The fulfillment of this condition notably simplifies the extraction of the kinetic information from the cyclic voltammetric data.<sup>14b</sup> Since the glucose concentration is constant throughout the reaction-diffusion layer and since the enzyme can be considered immobile as compared to the mediator (the enzyme has a diffusion coefficient of ca.  $4 \times 10^{-7}$  cm<sup>2</sup> s<sup>-1</sup>,<sup>15a</sup> whereas the ferrocenes have diffusion coefficients around  $7 \times 10^{-6}$  cm<sup>2</sup> s<sup>-1</sup>,<sup>15b,c</sup>), the only species that are engaged in both diffusional and chemical processes are the reduced and oxidized forms, P and Q, of the mediator. The sum of the concentrations of P and Q are equal to the bulk concentration of P,  $C_p^0$ , at any time throughout the reaction-diffusion layer. The current response may thus be obtained from the resolution of eq I, accompanied by the following initial and limiting conditions

$$t = 0, x \geq 0 \text{ and } x = \infty, t \geq 0 \quad [Q] = 0$$

$$x = 0, t \geq 0 \quad [Q] = \frac{C_p^0}{1 + \exp\left(\frac{E}{RT}(E - E^0)\right)}$$

( $E$  = electrode potential;  $E^0$  = standard potential of the mediator couple). The anodic current  $i$  flowing through the electrode surface is obtained from the gradient of Q at the electrode surface according to

$$i = -FSD \left( \frac{\partial [Q]}{\partial x} \right)_{x=0}$$

( $S$  = electrode surface area). The electrode potential is related to time during the anodic scan through

$$E = E_i + vt$$

( $E_i$  = starting potential;  $v$  = scan rate).

It is convenient to render the above formulation dimensionless by means of the following changes in variables and parameters

$$\tau = \frac{Fv}{RT}t \quad \xi = \frac{F}{RT}(E - E_i)$$

Thus:  $\tau = \xi + u$ , with

$$u = -\frac{F}{RT}(E_i - E^0)^{16}$$

$$y = x \left( \frac{Fv}{RT} \right)^{1/2} \quad q = \frac{[Q]}{C_p^0}$$

$$\lambda = \frac{2k_3 C_E^0}{v} \frac{RT}{F} \quad \text{(II)}$$

$$\sigma = \frac{k_3 C_p^0}{k_2} \left( 1 + \frac{k_{-1} + k_2}{k_1 C_G^0} \right) \quad \text{(III)}$$

Thus

$$\frac{\partial q}{\partial \tau} = \frac{\partial^2 q}{\partial y^2} - \frac{\lambda q}{1 + \sigma q} \quad \text{(IV)}$$

$$\text{with } \tau = 0, y \geq 0 \text{ and } y = \infty, \tau \geq 0 \quad q = 0 \quad \text{(V)}$$

$$y = 0, \tau \geq 0 \quad q = \frac{1}{1 + \exp(-\xi)} \quad \text{(VI)}$$

The current is obtained from the gradient of  $q$  at the electrode surface

$$i = FSC_p^0 \left( \frac{DFv}{RT} \right)^{1/2} \left( \frac{\partial q}{\partial y} \right)_{y=0} \quad \text{(VII)}$$

The resulting anodic current-potential curves all exhibit a plateau. For small values of  $\lambda$  they also exhibit a peak, whereas for large values of  $\lambda$  the peak vanishes. At the level of the plateau,  $\partial q / \partial \tau = 0$ , and simple integration of the system of eqs IV–VII leads to the following close-form expression of the plateau current

$$\frac{i_p}{i_p^0} = \frac{\lambda^{1/2}}{0.446} \left\{ 2 \left[ 1 - \frac{1}{\sigma} \ln(1 + \sigma) \right] \right\}^{1/2} \quad \text{(VIII)}$$

where  $i_p$  is the catalytic plateau current and  $i_p^0$  is the peak current of the reversible wave of the mediator in the absence of glucose,  $i_p^0$  is proportional to the square root of the scan rate<sup>14b</sup>

$$i_p^0 = 0.446 FSC_p^0 \left( \frac{DFv}{RT} \right)^{1/2}$$

and, thus,  $i_p$  is independent of the scan rate. The computation of the peak current when there is a peak is also useful for treating the case in which catalysis is weak. The ratio  $i_p/i_p^0$  (where  $i_p$  is now the peak current when there is a peak or the plateau current when the peak has disappeared) was calculated as a function of the parameters  $\lambda$  and  $\sigma$  by means of the Crank–Nicholson finite difference method<sup>17</sup> using previously described procedures.<sup>14b</sup>

The working curves relating the ratio  $i_p/i_p^0$  to the two parameters  $\lambda$  and  $\sigma$  are represented in Figure 2. For each value of  $\sigma$ , the  $i_p/i_p^0$  ratio tends toward unity as  $\lambda \rightarrow 0$  and toward the values given by the close-form eq VIII when  $\lambda \rightarrow \infty$ . Provided catalysis

(13) De Baetselier, A.; Vasavada, A.; Dohet, P.; Ha-Thi, V.; De Beukelaer, M.; Ercicum, T.; De Clerck, L.; Hanotier, J.; Rosenberg, S. *Biotechnology* **1991**, *9*, 559.

(14) (a) Savéant, J.-M.; Vianello, E. In *Advances in Polarography*; Longmair, I. S., Ed.; Pergamon Press: London, 1960; Vol. 1, pp 367–374. (b) Andrieux, C. P.; Savéant, J.-M. In *Electrochemical Reactions in Investigation of Rates and Mechanisms of Reactions, Techniques of Chemistry*; Bernasconi, C. F., Ed.; Wiley: New York, 1986; Vol. VI/4E, Part 2, pp 305–390.

(15) (a) Swoboda, B. E. P.; Massey, V. *J. Biol. Chem.* **1965**, *240*, 2209. (b) Oshawa, Y.; Aoyagui, S. *J. Electroanal. Chem.* **1978**, *86*, 289. (c) Bond, A. M.; McLennan, E. A.; Stojanovic, R. S.; Thomas, F. G. *Anal. Chem.* **1987**, *59*, 2853.

(16) Practically,  $u = \infty$  since the starting potential is poised at the foot of the wave, where the current flowing through the electrode is negligible.

(17) Crank, J. *Mathematics of Diffusion*; Oxford University Press: London, 1964.

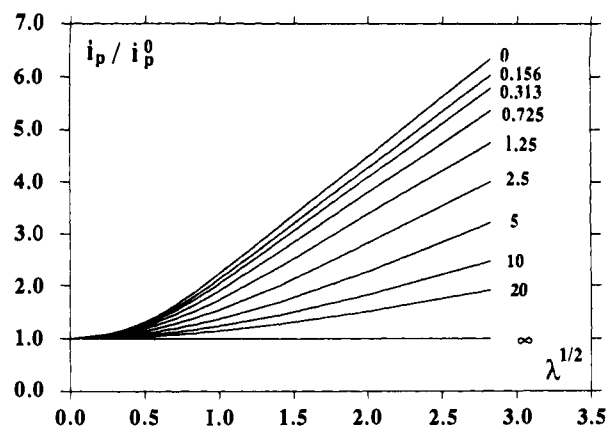


Figure 2. Theoretical dependence of the peak and plateau current ratio,  $i_p/i_p^0$ , with the parameters  $\lambda = (2k_3C_E^0/v)$  and  $\sigma = (k_3C_p^0/k_2)\{1 + [(k_2 + k_2)k_1C_G^0]\}$ . The number of each curve is the value of  $\sigma$ .

Table I. One-Electron Mediators

mediator (reduced form)	standard potential (V vs SCE)
ferrocenemethanol	0.190
ferrocenecarboxylate	0.290
(( <i>N,N</i> -dimethylamino)methyl)ferrocene (ammonium form)	0.370
promazine (ammonium form)	0.530

is not too strong, these two limiting behaviors can be reached by increasing and decreasing the scan rate, respectively ( $\lambda$  is inversely proportional to  $v$ ). The first-order behavior we have evoked earlier corresponds to  $\sigma \rightarrow 0$ , i.e., to the upper curve in Figure 2. A convenient manner for reaching this limit is to decrease the bulk concentration of the reduced form of the mediator,  $C_p^0$  ( $\sigma$  is proportional to  $C_p^0$ ).

With the native enzyme, we have investigated the kinetics of the catalytic reaction as a function of pH with the one-electron mediators listed in Table I. Catalysis by the recombinant enzyme was investigated with ferrocenemethanol as the mediator.

For each value of the concentrations of glucose, enzyme, and mediator and each pH, the catalytic wave was examined as a function of the scan rate. For each concentration of glucose and mediator, the concentration of enzyme was adjusted so as to be small enough for complete reversibility of the cyclic voltammogram to be obtained easily upon raising the scan rate and large enough for the catalytic increase of the current to be sufficient for authorizing an accurate determination of the overall rate constant. Moreover, the ratio  $C_p^0/C_E^0$  was always made larger than 50 in order to ensure the applicability of the steady-state approximation to all the possible enzyme forms in the detailed analysis of the catalysis kinetics.

Figure 3 shows a first example of the variations of the peak current with the scan rate, obtained at high glucose concentration with the ferrocene methanol mediator for a series of pH and, at each pH, for several values of the concentration of mediator (the stability of both forms of the mediator couple in the whole pH range is attested by the reversibility of the cyclic voltammogram wave and the constancy of the standard potential). In all cases, the ratio  $i_p/v^{1/2}$  tends toward a limit as  $v$  increases, corresponding to  $i_p^0$  (reversibility of the mediator wave). The vertical axis in Figure 3 has been thus normalized toward the value of  $i_p^0$  in each case. As the horizontal axis for each curve we have taken  $(C_E^0/v)^{1/2}$  in order to compare the experimental data with the  $i_p/i_p^0$  vs  $\lambda^{1/2}$  theoretical curves (Figure 2),  $\lambda$  being proportional to  $C_E^0/v$  (eq II). At the highest pH, it is apparent that the experimental  $i_p/i_p^0$  vs  $(C_E^0/v)^{1/2}$  curves tend toward the behavior expected for  $\sigma \rightarrow 0$ , i.e., featuring first-order conditions, as  $C_p^0$  is made smaller and smaller. The values of  $C_p^0$  at which the first-order behavior is reached are larger and larger as the pH is decreased. Since the parameter  $\sigma$  is proportional to  $k_3C_p^0$  (eq II), this is consistent with the observation that the overall rate constant  $k_3$  decreases

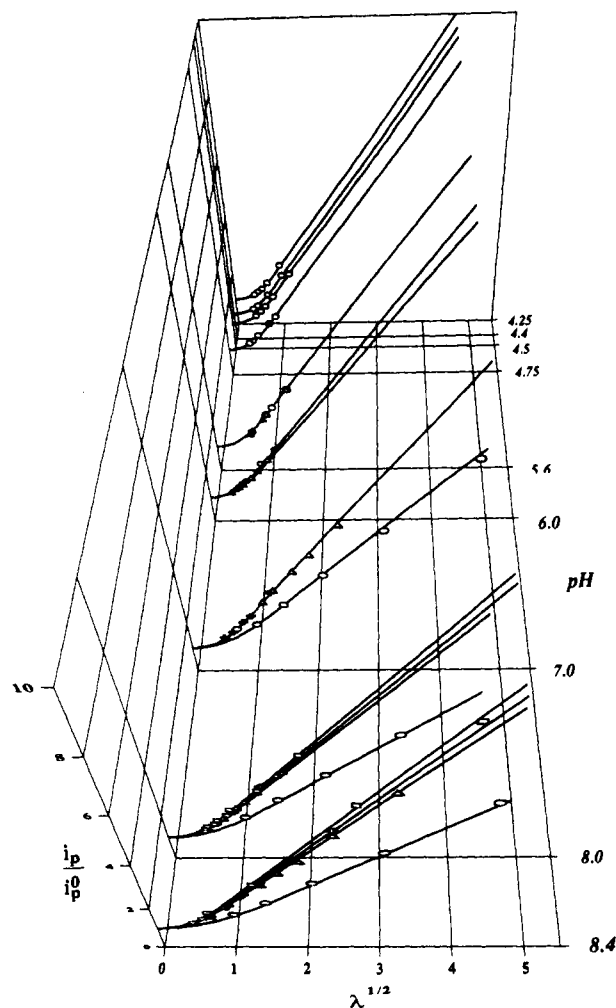


Figure 3. Catalysis of the electrochemical oxidation of glucose by native glucose oxidase mediated by ferrocenemethanol. Variations of the anodic cyclic voltammogram peak or plateau current with the scan rate, the mediator concentration, and the pH. Ionic strength = 0.1 M; temperature = 25 °C; mediator concentrations in  $\mu\text{M}$ : 2.5 ( $\square$ ), 5 ( $\square$ ), 10 ( $\Delta$ ), 100 ( $\circ$ ). The experimental data (points) are fitted with the working curves (full lines) by adjusting the experimental abscissa axis  $(C_E^0/v)^{1/2}$  to the theoretical abscissa axis  $\lambda^{1/2}$  (eq II) with the following values of  $k_3$  ( $\times 10^{-5} \text{ M}^{-1} \text{ s}^{-1}$ )

pH	4.25	4.4	4.5	4.75	5.6	6.0	7.0	8.0	8.4
$k_3$	0.7	0.9	1.2	1.5	6.0	11.5	60	110	120

with the pH. From the fitting of the experimental curves corresponding to the first-order conditions by the  $\sigma = 0$  theoretical curves, one immediately obtains the value of  $k_3$  at each pH.

Similar experiments were carried out with the three other mediators and the native enzyme (Figures 4–6), limiting the pH to values smaller than 7 for the ammonium form of ((*N,N*-dimethylamino)methyl)ferrocene so as to keep the amino group protonated, smaller than 5.5 for promazine for the same reason, and larger than 5.6 so as to keep the carboxylate group unprotonated (the  $E^0$  of each couple remains constant in the pH range investigated). The same treatment of the  $i_p/i_p^0 - (C_E^0/v)^{1/2}$  curves and of their variations with  $C_p^0$  allowed for the determination of  $k_3$  in all cases.

Turning back to ferrocenemethanol, we have investigated the possible effect of the concentration of base present in the buffer at pH = 6. Figure 7 shows the experimental results. Varying the concentration of  $\text{HPO}_4^{2-}$  from 2.8 to 11 mM (while keeping the ionic strength constant and equal to 0.1 M by addition of  $\text{Na}_2\text{SO}_4$ ) did not result in any noticeable effect of the buffer concentration on the value of  $k_3$ .

The variations of  $k_3$  with the pH for each of the four mediators are summarized in Figure 8.

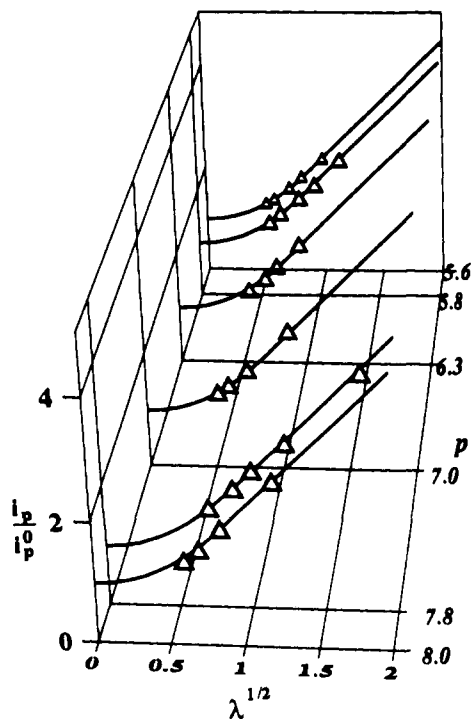


**Figure 4.** Catalysis of the electrochemical oxidation of glucose by native glucose oxidase mediated by ferrocenecarboxylate. Variations of the anodic cyclic voltammetric peak or plateau current with the scan rate, the mediator concentration, and the pH. Ionic strength = 0.1 M; temperature = 25 °C; mediator concentration = 20  $\mu$ M. The experimental data ( $\Delta$  points) are fitted with the working curves (full lines) by adjusting the experimental abscissa axis  $(C_E^0/v)^{1/2}$  to the theoretical abscissa axis  $\lambda^{1/2}$  (eq II) with the following values of  $k_3$  ( $\times 10^{-5} \text{ M}^{-1} \text{ s}^{-1}$ )

pH	5.6	5.8	6.3	7.0	7.8	7.8 <sub>s</sub>
$k_3$	0.55	0.65	0.85	1.5	2.1	2.2

**Table II.** Rate Constants of the Reductive Half-Reaction for the Native and Recombinant Glucose Oxidases<sup>a,b</sup>

pH	$k_{\text{red}}$ ( $\text{M}^{-1} \text{ s}^{-1}$ )	$k_2$ ( $\text{s}^{-1}$ )
6.0	$1.5 \times 10^4$ ( $1.3 \times 10^4$ )	1050
7.0	$1.2 \times 10^4$ ( $1.32 \times 10^4$ )	780
8.0	$1.1 \times 10^4$ ( $1.1 \times 10^4$ )	680
8.0 <sup>c</sup>	$0.95 \times 10^4$	770

<sup>a</sup> Phosphate buffers; ionic strength = 0.1 M; temperature = 25 °C.

<sup>b</sup> Between parentheses are values obtained with dioxygen as cosubstrate.<sup>5a</sup> <sup>c</sup> Recombinant enzyme.

As seen above, the kinetics tend to deviate from the first-order conditions upon increasing the mediator concentration,  $C_p^0$ . A way of amplifying this effect is to decrease the glucose concentration,  $C_G^0$ , since, as can be seen from eq III, a decrease of  $C_G^0$  induces an increase of  $\sigma$ . We have taken advantage of this effect to determine the kinetic characteristics of the reductive half-reaction. Figure 9 shows the  $i_p/i_0p - (C_E^0/v)^{1/2}$  curves obtained with a concentration of 0.1 mM of the ferrocenemethanol mediator as a function of glucose concentration in the range of 5–500 mM.

The ensuing variations of the parameter  $\sigma/k_3 C_p^0$  with the inverse of glucose concentration are shown in Figure 10. As predicted, the plots are linear. The intercepts provide the value of  $1/k_2$ , and the slopes give that of  $(k_{-1} + k_2)/k_1 k_2$ . The resulting values of  $k_2$  and  $k_{\text{red}} = k_1 k_2 / (k_{-1} + k_2)$  are summarized in Table II.

The same approaches were also used to determine the oxidation rate constant and the rate constants of the reductive half-reaction with the recombinant enzyme at pH = 8, using ferrocenemethanol as a mediator (Figure 11). The results are shown in Figure 8 and Table II.

## Discussion

With the exception of promazine, which may have been investigated in too narrow a range of pH, the overall rate constant

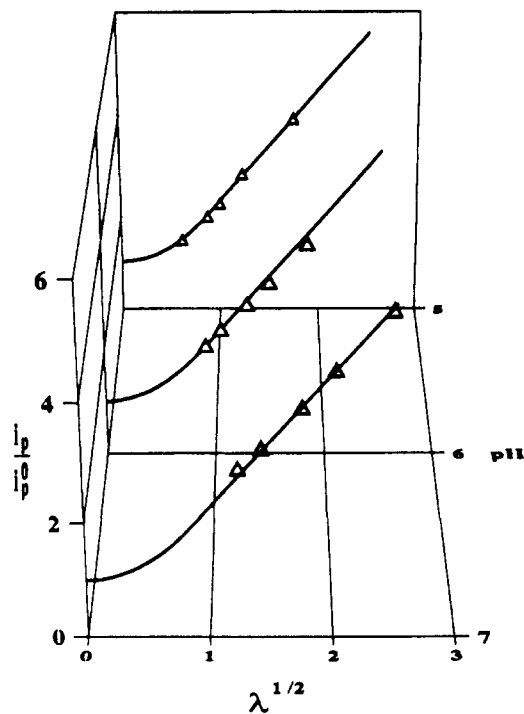


**Figure 5.** Catalysis of the electrochemical oxidation of glucose by native glucose oxidase mediated by ((dimethylammonio)methyl)ferrocenecarboxylate. Variations of the anodic cyclic voltammetric peak or plateau current with the scan rate and the pH. Ionic strength = 0.1 M; temperature = 25 °C; mediator concentrations = 10  $\mu$ M. The experimental data ( $\Delta$  points) are fitted with the working curves (full lines) by adjusting the experimental abscissa axis  $(C_E^0/v)^{1/2}$  to the theoretical abscissa axis  $\lambda^{1/2}$  (eq II) with the following values of  $k_3$  ( $\times 10^{-5} \text{ M}^{-1} \text{ s}^{-1}$ )

pH	5.0	6.0	7.0
$k_3$	5.5	33	100

$k_3$  clearly varies with pH in all cases (Figure 8).

Reaction 3 is, in fact, a multistep reaction during which two electrons and two protons are exchanged between the reduced form of the enzyme ( $\text{FADH}_2$ ) and two molecules of the mediator ( $Q$ ) and two molecules of the base (noted B, whatever its charge) contained in the buffer. The following reaction scheme is a representation of the  $2e^- + 2H^+$  process ultimately leading to the oxidized form of the enzyme, FAD. In the succession of reactions, the proton transfers 7 and 10 may be considered as remaining at equilibrium, since we have observed that the overall kinetics are independent of the buffer concentration. In Scheme II we have also allowed for the possibility that the mediator molecules may form a precursor complex with the enzymatic site.

Reactions 5 and 12 are regarded as irreversible both because they are down-hill processes (the standard potentials of the  $\text{FADH}_2/\text{FADH}_2^{*+}$  and  $\text{FADH}^+/\text{FADH}^{*+}$  couples can be estimated to be  $-0.07$  and  $-0.09$  V vs SCE,<sup>18</sup> whereas the smallest standard potential in the series of mediators is 0.190 V vs SCE) and because the  $\text{FADH}_2^{*+}$  and  $\text{FADH}^{*+}$  cations they generate are strong acids ( $\text{p}K_a = 2$  and 0, respectively<sup>18</sup>). Reactions 9 and 15 are likewise regarded as irreversible because they are strongly down-hill (the standard potentials of the  $\text{FADH}^-/\text{FADH}^*$  and  $\text{FAD}^{*+}/\text{FAD}$  couples are  $-0.330$  and  $-0.520$  V vs SCE, respectively<sup>18</sup>).

Under these conditions, the kinetic term in eq IV is defined by means of the following equations

(18) (a) These values, taken or derived from refs 11a,b and 18b–d, are for the free flavin. As far as we are dealing with qualitative trends, their use instead of those of the enzyme-bound flavin is legitimate: for example, the  $\text{FAD}^{*+}/\text{FAD}$  couple has a standard potential of 0.445 in the enzyme instead of 0.520 in the free flavin. (b) Lowe, H. J.; Clark, W. M. *J. Biol. Chem.* 1956, 221, 993. (c) Hemmerich, P.; Veeger, C.; Wood, H. C. S. *Angew. Chem., Int. Ed. Engl.* 1965, 4, 671. (d) Janik, B.; Elving, P. J. *Chem. Rev.* 1968, 68, 295.

$$\frac{1}{k_3} = \frac{1 + \frac{K_{a,7}}{[H^+]}}{\frac{k_4 k_5}{k_{-4} + k_5} + \frac{K_{a,7} k_8 k_9}{[H^+] k_{-8} + k_9}} + \frac{1 + \frac{K_{a,10}}{[H^+]}}{\frac{k_{11} k_{12}}{k_{-11} + k_{12}} + \frac{K_{a,10} k_{14} k_{15}}{[H^+] k_{-14} + k_{15}}} \quad (\text{IX})$$

$$\sigma = k_3 C_p^0 \left[ \frac{\frac{k_4}{k_{-4} + k_5} + \frac{K_{a,7} k_8}{[H^+] k_{-8} + k_9}}{\frac{k_4 k_5}{k_{-4} + k_5} + \frac{K_{a,7} k_8 k_9}{[H^+] k_{-8} + k_9}} + \frac{\frac{k_{11}}{k_{-11} + k_{12}} + \frac{K_{a,10} k_{14}}{[H^+] k_{-14} + k_{15}}}{\frac{k_{11} k_{12}}{k_{-11} + k_{12}} + \frac{K_{a,10} k_{14} k_{15}}{[H^+] k_{-14} + k_{15}}} + \frac{1}{k_2} + \frac{k_{-1} + k_2}{k_1 k_2} \frac{1}{C_G^0} \right] \quad (\text{X})$$

where  $K_{a,7}$  and  $K_{a,10}$  are the acidity constants of  $\text{FADH}_2$  and  $\text{FADH}^*$ , respectively.

Upon decreasing the pH, these equations tend toward

$$\frac{1}{k_3} = \left( \frac{1}{k_4} + \frac{1}{K_4 k_5} \right) + \left( \frac{1}{k_{11}} + \frac{1}{K_{11} k_{12}} \right)$$

$$(K_4 = k_4/k_{-4}; K_{11} = k_{11}/k_{-11})$$

$$\sigma = k_3 C_p^0 \left( \frac{1}{k_5} + \frac{1}{k_{12}} + \frac{1}{k_2} + \frac{k_{-1} + k_2}{k_1 k_2} \frac{1}{C_G^0} \right)$$

and upon increasing the pH

$$\frac{1}{k_3} = \left( \frac{1}{k_8} + \frac{1}{K_8 k_9} \right) + \left( \frac{1}{k_{14}} + \frac{1}{K_{14} k_{15}} \right)$$

$$(K_8 = k_8/k_{-8}, K_{14} = k_{14}/k_{-14})$$

$$\sigma = k_3 C_p^0 \left( \frac{1}{k_9} + \frac{1}{k_{15}} + \frac{1}{k_2} + \frac{k_{-1} + k_2}{k_1 k_2} \frac{1}{C_G^0} \right)$$

In view of the driving forces of the electron-transfer steps, there is little doubt that  $k_5, k_{12}, k_9, k_{15} \gg k_2$  and thus that eq X simplifies to eq III within all the experimental conditions we have investigated. The validity of this approximation is confirmed by the quite satisfactory agreement between the values found here for these parameters and those found before using an entirely different cosubstrate, dioxygen (see Table II). The use of eq III for obtaining the kinetic parameters of the reductive half-reaction, as done in the Results section, is thus entirely justified.

As seen from the variations of  $k_3$  with the  $\text{pH}^{19}$  with ferrocenemethanol and ferrocenecarboxylate (Figure 8), the  $\text{p}K_a$ s in-

(19) These results seem to contrast those of previous studies<sup>8a,b</sup> in which the rate constant was concluded to be independent of pH, not only with ferrocenecarboxylate, where the variation we find is not very ample, but also with ferrocenemethanol and ((dimethylammonio)methyl)ferrocene, where a large variation is found. In fact, this discrepancy derives from the fact that the first-order approximation was used systematically in these previous studies even under conditions where it does not apply, in particular when  $k_3$  is large (see eq 11). For the highest values of  $k_3$  found here with ferrocenemethanol and ((dimethylammonio)methyl)ferrocene,  $\sigma$  reaches values as high as 30, resulting in an underestimation of  $k_3$  by a factor of ca. 30 when the data are analyzed under the first-order approximation. Since  $k_3$  decreases with the pH, its first-order approximation estimate is less and less erroneous. The net result is thus a cancellation of the variation with pH. The first-order approximation is much closer to the truth with ferrocenecarboxylate where  $k_3$  is much smaller. To detect the relatively small variation of  $k_3$  with pH, represented in Figure 8, it was necessary to carry out a careful analysis of the effect of scan rate under conditions where the catalytic effects are small. It was then mandatory to treat the experimental data by means of the complete finite difference simulation analysis we have described.

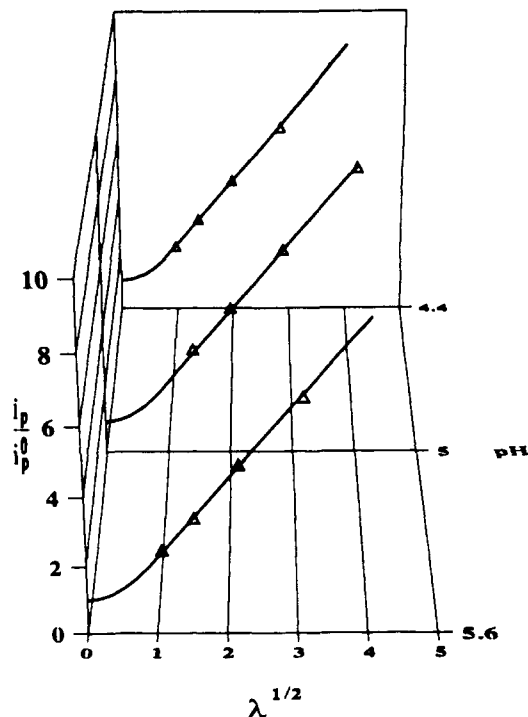


Figure 6. Catalysis of the electrochemical oxidation of glucose by native glucose oxidase mediated by the promazine dication radical. Variations of the anodic cyclic voltammetric peak or plateau current with the scan rate and the pH. Ionic strength = 0.1 M; temperature = 25 °C; mediator concentration = 50  $\mu\text{M}$ . The experimental data ( $\Delta$  points) are fitted with the working curves (full lines) by adjusting the experimental abscissa axis  $\lambda^{1/2} (C_E^0/b)^{1/2}$  to the theoretical abscissa axis  $\lambda^{1/2}$  (eq II) with the following values of  $k_3$  ( $\times 10^{-5} \text{ M}^{-1} \text{ s}^{-1}$ )

pH	4.4	5.0	5.6
$k_3$	28	30	28

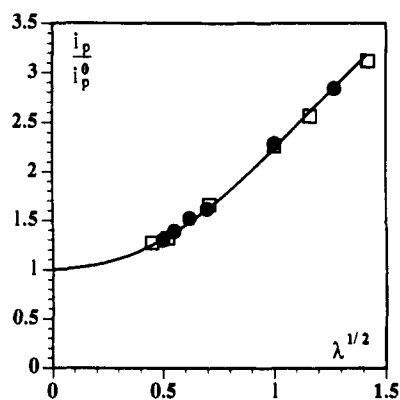
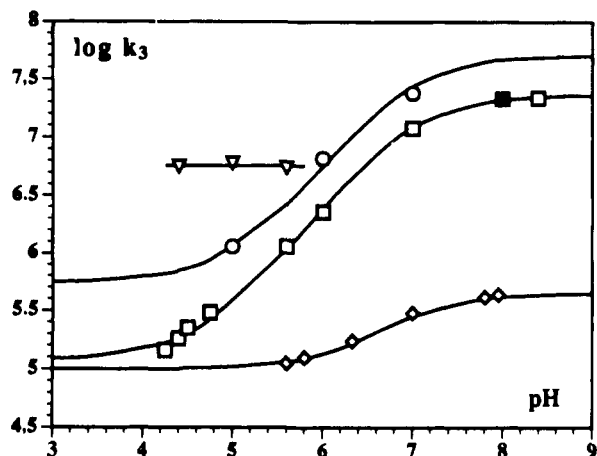


Figure 7. Catalysis of the electrochemical oxidation of glucose by native glucose oxidase mediated by ferrocenemethanol. Effect of the concentration of base in the buffer:  $[\text{HPO}_4^{2-}]$  (mM) = 2.5 ( $\square$ ), 11 ( $\bullet$ ); pH = 6; ionic strength = 0.1 M (adjusted by addition of  $\text{Na}_2\text{SO}_4$ ); temperature = 25 °C. The experimental data (points) are fitted with the working curves (full lines) by adjusting the experimental abscissa axis  $(C_E^0/b)^{1/2}$  to the theoretical abscissa axis  $\lambda^{1/2}$  (eq II) with the following values of  $k_3$

$[\text{HPO}_4^{2-}]$ (mM)	2.5	11
$k_3 \times 10^{-5} (\text{M}^{-1} \text{ s}^{-1})$	12.5	12.5

involved are in the vicinity of 7, as are the  $\text{p}K_a$ s of the  $\text{FADH}_2/\text{FADH}^-$  and  $\text{FADH}^*/\text{FADH}^-$  acid-base couples (6.6 and 7.6, respectively, as can be derived from the equilibrium data reported in ref 12a or 7.3 for the  $\text{FADH}^*/\text{FADH}^-$  from more direct spectral studies<sup>12a</sup>). This observation indicates that these variations are not caused by electrostatic interactions between the charge on the mediator and the global negative charge borne by the enzyme which has an isoelectric point of ca. 4.0.<sup>20</sup> This conclusion falls



**Figure 8.** Catalysis of the electrochemical oxidation of glucose by native and recombinant glucose oxidase mediated by one-electron redox co-substrates. Variation of the oxidation rate constant  $k_3$  with pH. Ionic strength = 0.1 M; temperature = 25 °C; native enzyme + ferrocenemethanol (□), + ferrocenecarboxylate (◇), + ((dimethylammonio)methyl)ferrocene (○), + promazine dication radical (▽). Recombinant enzyme + ferrocenemethanol (×).

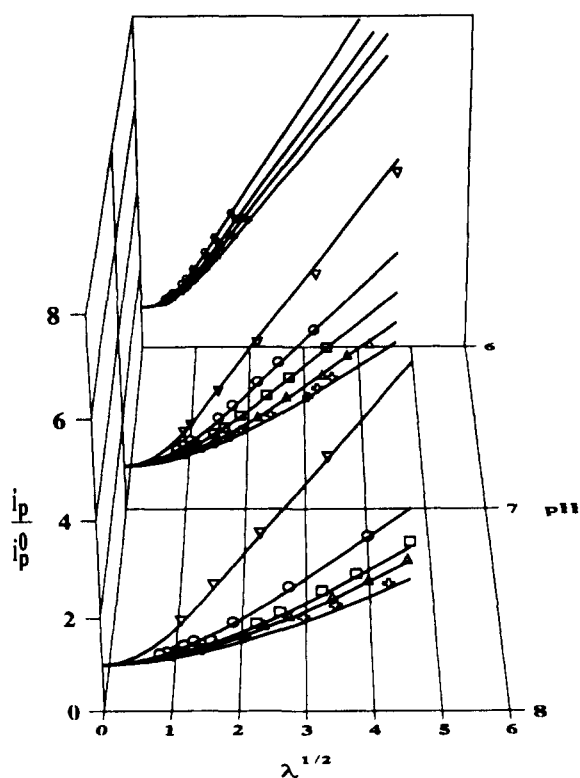


**Figure 9.** Catalysis of the electrochemical oxidation of glucose by native glucose oxidase mediated by ferrocenemethanol. Variations of the anodic cyclic voltammetric peak or plateau current with the scan rate, the glucose concentration, and the pH. Ionic strength = 0.1 M; temperature = 25 °C; glucose concentrations in mM: 5 (◇), 6.7 (Δ), 10 (□), 20 (○), 500 (▽). The experimental data (points) are fitted with the working curves (full lines) by adjusting the experimental abscissa axis  $(C_E^0/v)^{1/2}$  to the theoretical abscissa axis  $\lambda^{1/2}$  (eq II) with the following values of  $k_3$  ( $\times 10^{-5} \text{ M}^{-1} \text{ s}^{-1}$ )

pH	6.0	7.0	8.0
$k_3$	11.5	60	110

in line with the fact that the ionic strength (0.1 M) appears to be large enough for the charge on the mediator and the charge of the enzyme to be almost entirely shielded by the ions present in the solution.<sup>21</sup>

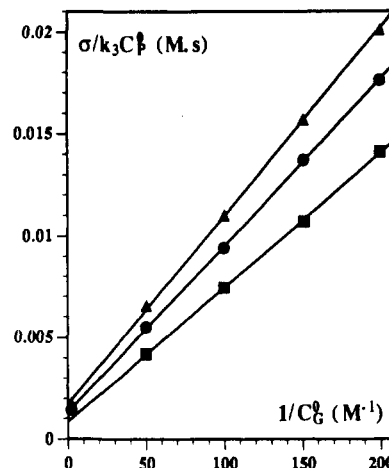


**Figure 10.** Catalysis of the electrochemical oxidation of glucose by native glucose oxidase mediated by ferrocenemethanol. Determination of the rate constants of the reductive half-reaction. Variation of the parameter  $\sigma/k_3C_p^0$  with  $1/C_G^0$ . Ionic strength = 0.1 M; temperature = 25 °C; pH = 6.0 (■), 7.0 (●), 8.0 (▲).

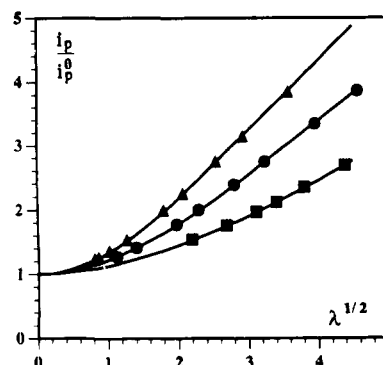


**Figure 11.** Catalysis of the electrochemical oxidation of glucose by the recombinant enzyme mediated by ferrocenemethanol at pH 8.0. Variations of the anodic cyclic voltammetric peak or plateau current with the scan rate and the glucose concentration. Ionic strength = 0.1 M; temperature = 25 °C; glucose concentrations in mM: 21.7 (▲), 11.6 (●), 5 (■). The experimental data (points) are fitted with the working curves (full lines) by adjusting the experimental abscissa axis  $(C_E^0/v)^{1/2}$  to the theoretical abscissa axis  $\lambda^{1/2}$  (eq II) with  $k_3 = 1.1 \times 10^7 \text{ M}^{-1} \text{ s}^{-1}$ .

**Table III.** Driving Forces of the Electron-Transfer Reactions (in meV)<sup>a</sup>

reaction	ferrocene methanol	ferrocene carboxylate	((dimethylamino)methyl)ferrocene	promazine
5	260	360	440	600
12	280	380	460	620
9	520	620	700	860
15	710 (635)	810 (735)	890 (815)	1050 (975)

<sup>a</sup> From the standard potentials of the free flavin; between parentheses values are from the standard potential of the enzyme-bound flavin.<sup>18</sup>

The driving forces of the four electron-transfer steps (5, 12, 9, 15) in the scheme are summarized in Table III. From these values we may consider that  $k_9 \approx k_{12}$  and  $k_9 \approx k_{15}$  for each mediator. The binding and dissociation rate constants to and from the enzyme site are likely to be close, one to the other, for  $\text{FADH}_2$ ,  $\text{FADH}^\cdot$ ,  $\text{FADH}^+$ , and  $\text{FAD}^{\cdot-}$ . The  $\text{pK}_a$  of the  $\text{FADH}_2/\text{FADH}^\cdot$  and  $\text{FADH}^\cdot/\text{FAD}^{\cdot-}$  couples are also close. We may thus fit the variations of the overall rate constant  $k_3$  with the pH for ferrocenemethanol and ferrocenecarboxylate under these simplifying assumptions (see Figure 8).

(20) Voet, J. G.; Coe, J.; Epstein, J.; Matossian, V.; Shipley, T. *Biochemistry* 1981, 20, 7182.

(21) Feinberg, B. A.; Ryan, M. D. *J. Org. Biochem.* 1981, 15, 187.

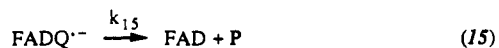
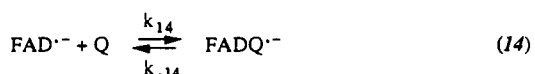
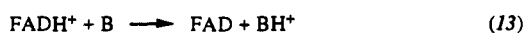
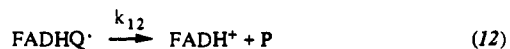
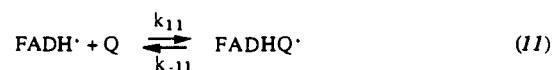
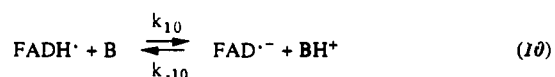
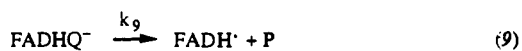
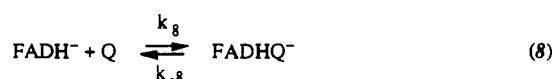
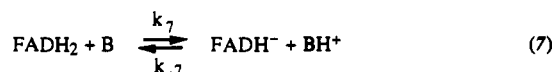
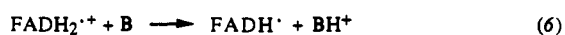
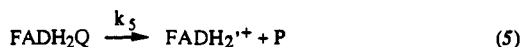
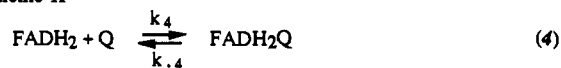


Table IV. Rate Constants of Electron Transfers<sup>a</sup>

	ferrocene methanol	ferrocene carboxylate	((dimethylamino)- methyl)ferrocene	promazine
$\log \frac{k_4 k_5}{k_{-4} + k_5} \approx \log \frac{k_{10} k_{11}}{k_{-10} + k_{11}}$	5.1	5.0	≈5.7	6.8
$\log \frac{k_8 k_9}{k_{-8} + k_9} \approx \log \frac{k_{14} k_{15}}{k_{-14} + k_{15}}$	7.4	5.6	≈7.7	

<sup>a</sup>In M<sup>-1</sup> s<sup>-1</sup>.

## Scheme II



In both cases, we find from the best fitting of the experimental data a value of 7 for the average of the FADH<sub>2</sub>/FADH<sup>-</sup> and FADH<sup>·</sup>/FAD<sup>·-</sup> pK<sub>a</sub>s. This is in good agreement with previous spectrophotometric data.<sup>12a</sup> It is also seen that the variation of k<sub>3</sub> with pH in the case of the ammonium form of ((dimethylamino)methyl)ferrocene, although investigated within a narrower range of pH, is consistent with this pK<sub>a</sub> value.

We may also derive from these fittings approximate values for the rate constants of the electron-transfer reactions (Table IV).

It clearly appears (Table IV) that there is no simple correlation between the rate constants and the driving forces of the corresponding reactions (Table III). Regarding, for example, the FADH<sup>-</sup> → FADH<sup>·</sup>, FAD<sup>·-</sup> → FAD reaction, the ferrocene-carboxylate mediator is much slower than ferrocenemethanol in spite of a 100-meV driving force advantage. The ammonium form of ((dimethylamino)methyl)ferrocene is only twice more reactive than ferrocenemethanol in spite of a driving force advantage of 180 meV. These observations point to the formation of a precursor complex between the mediator and the enzyme site, the energetics and/or kinetics of which may influence the kinetics of the electron transfer as depicted in the reaction scheme and rate analysis

described above. The very fact that the observed rate constants are much below the bimolecular diffusion limit<sup>22</sup> for such large driving forces (Table III) indicates that an energetically unfavorable formation of a precursor complex (steps 4, 8, 11, 14) precedes the electron transfer itself (steps 5, 9, 12, 15). Since the driving forces of the latter reactions are large, it may well be that the formation of the precursor complex is then, or is then close to being, the rate-determining step of the overall electron-transfer reaction. A histidine residue or a thiol group located in the close vicinity of the flavin would be likely candidates for the binding site.<sup>23</sup> It thus appears that the formation of the precursor complex is less favorable with ferrocenecarboxylate than with ferrocenemethanol and the ammonium form of ((dimethylamino)methyl)ferrocene.

The oxidation of the protonated forms, FADH<sub>2</sub> and FADH<sup>·</sup>, proceeds with a lesser driving force than that of FADH<sup>-</sup> and FAD<sup>·-</sup> (Table III). There is thus a tendency for the electron-transfer reactions to be controlled by the electron-transfer step itself and thus to follow more closely the driving forces, as appears when comparing ferrocenemethanol, ((dimethylammonio)methyl)ferrocene, and promazine. In this framework, the almost equal rate constants found for ferrocenemethanol and ferrocenecarboxylate would result in a compensation of the driving force advantage of the second mediator over the first by the more difficult formation of the precursor complex we have already noted (k<sub>4</sub> ≈ k<sub>8</sub> ≈ k<sub>11</sub> ≈ k<sub>14</sub> and k<sub>4</sub>/k<sub>-4</sub> ≈ k<sub>8</sub>/k<sub>-8</sub> ≈ k<sub>11</sub>/k<sub>-11</sub> ≈ k<sub>14</sub>/k<sub>-14</sub> would be smaller for ferrocenecarboxylate than for ferrocenemethanol).

The values of the rate constants we have found at pH = 8 with ferrocenemethanol in the case of the recombinant enzyme (k<sub>2</sub> = 770 vs 680 s<sup>-1</sup>, k<sub>red</sub> = 0.95 × 10<sup>4</sup> vs 1.1 × 10<sup>4</sup> M<sup>-1</sup> s<sup>-1</sup>, k<sub>3</sub> = 1.2 × 10<sup>7</sup> vs 1.2 × 10<sup>7</sup> M<sup>-1</sup> s<sup>-1</sup>) are practically the same as those with the native enzyme. The catalytic activity is thus insensitive to the extensive glycosylation that has taken place in the recombinant enzyme, as found with dioxygen as the cosubstrate.<sup>4c</sup> The thick carbohydrate layer, therefore, appears sufficiently permeable to both the substrate and the cosubstrate so as not to introduce any additional rate limitation in the catalytic process.

## Experimental Section

**Materials.** The various ferrocenes, promazine, glucose, and glucose oxidase from *A. niger* were commercial products from Strem Chemicals, Sigma, Prolabo, and Boehringer Mannheim (grade I), respectively. Overglycosylated glucose oxidase, produced from *Saccharomyces cerevisiae*, was a gift from the International Institute of Cellular Molecular Pathology of Brussels. The carbohydrate content of this recombinant enzyme was estimated to be 60–70% of the molecular weight.<sup>3,13</sup> The stock solutions of glucose were allowed to mutarotate overnight before use.

**Instrumentation.** The cyclic voltammetry working electrode was a glassy carbon (from Tokai Corp) disk of 3-mm diameter. It was carefully polished with diamond pastes (down to 1 μm) and ultrasonically washed before use. The instrument for cyclic voltammetry was composed of a function generator (Taccussel GSP4), a home-built potentiostat,<sup>24</sup> and a chart recorder (Iffelec).

A Hewlett-Packard HP 8452 spectrophotometer was used for the UV-visible assays of the enzyme concentration.

**Spectrophotometric Assay of the Enzyme Concentration.** For the stock solution of enzyme, we proceeded as described in ref 5, using as the

(22) This should be of the order of 10<sup>9</sup> M<sup>-1</sup> s<sup>-1</sup> in view of the good accessibility of the flavin site.<sup>9</sup>

(23) Nakanishi, Y.; Ohashi, K.; Tsuge, M. *Agric. Biol. Chem.* 1984, 48, 2951.

(24) Garreau, D.; Savéant, J. M. *J. Electroanal. Chem.* 1972, 35, 309.

differential extinction coefficient between oxidized and reduced form of the enzyme a value of  $13.1 \times 10^3 \text{ M}^{-1} \text{ cm}^{-1}$  at 450 nm.

### Conclusions

The main conclusions emerging from the present study may be summarized as follows.

When using one-electron redox cosubstrates, cyclic voltammetry may be efficiently applied to the simultaneous determination of the rate constants of both the reductive half-reaction and of the oxidation of the reduced enzyme. It suffices to create experimental conditions in which the kinetics of the catalytic reaction significantly deviate from first-order conditions and to treat the data accordingly. The determination of the oxidation rate constant may then be achieved by decreasing the mediator concentration so as to reach the first-order behavior under controlled conditions.

This procedure avoids the danger of significantly underestimating the oxidation rate constant when this is large. From this application, it is now possible to understand why glucose oxidase electrodes using positively charged ferrocenium mediators are insensitive to dioxygen. The oxidation rate constant thus found at pH = 7 is indeed larger than that observed with dioxygen.

Clear variations of the oxidation rate constants with pH have been found. They indicate that the  $pK_a$ s involved are those of

the  $\text{FADH}_2/\text{FADH}^\bullet$  and  $\text{FADH}^\bullet/\text{FAD}^{\bullet-}$  acid-base couples and may thus be rationalized by a kinetic scheme in which the various protonated and deprotonated forms present at the three successive oxidation states of the flavin are taken into account.

Analysis of the catalytic response in the most basic and most acidic sides of the pH range as a function of the electron-transfer driving force offered by the various mediators investigated points to the intermediacy of a precursor complex between the mediator and a site close to the flavin. The interference of the thermodynamics and kinetics of the formation of this precursor complex thus allows differentiation of the one-electron redox mediators by the enzyme.

It is also interesting to note that extensive glycosylation in the recombinant enzyme we have investigated left practically unaltered the catalytic activity for what is regarded as both the reductive half-reaction and the oxidation of the reduced form of the enzyme by the one-electron redox mediators.

**Acknowledgment.** We are grateful to Dr. A. de Baetselier (ICP-UCL, Brussel) for the generous gift of the recombinant glucose oxidase. We thank Dr. C. P. Andrieux (Laboratoire d'Electrochimie Moléculaire de l'Université de Paris VII) for his help in the numerical computations of eqs IV-VII.

## Potassium Cryptate Catalysis in the Elimination Reaction of a Sulfonate Ester

Marko J. Pregel and Erwin Bunzel\*

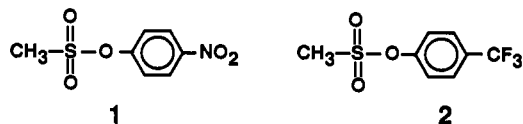
Contribution from the Department of Chemistry, Queen's University, Kingston, Ontario, K7L 3N6 Canada. Received June 1, 1992

**Abstract:** In the reaction of *p*-nitrophenyl methanesulfonate (1) with alkali-metal ethoxides, it is found that potassium ethoxide in the presence of excess 2.2.2 cryptand is more reactive than potassium ethoxide alone or in the presence of excess 18-crown-6. An upward curvature in the plot of  $k_{\text{obs}}$  vs  $[\text{KOEt}]_0$  in the presence of 2.2.2 cryptand is interpreted as arising from parallel reactions of free ethoxide ion and the ion pair of ethoxide ion with cryptated potassium ion ( $[\text{K} \subset 2.2.2]^+\text{EtO}^-$ ), the latter being more reactive than the former. It is shown that the ester reacts predominantly by an E1cb-type elimination mechanism, and the potassium cryptate appears to stabilize the transition state for leaving-group departure by electrostatic interactions through an 18-membered ring "window" in the cryptand.

### Introduction

We have been engaged in systematic studies of the mechanisms of reaction of alkali-metal ethoxides with carbon-, phosphorus-, and sulfur-based esters designed to reveal the effect of variation of both the alkali-metal ion and the nature of the substrate ester in these reactions. Our studies have revealed a spectrum of different metal ion effects, ranging from catalysis by all of the alkali-metal ions to inhibition by all.<sup>1</sup> Throughout these studies, crown ethers and cryptands were used to complex the metal ions in order to access the reactivity of free ethoxide ion. In the course of this work, we have discovered a system in which the 2.2.2 cryptate of potassium ion ( $\text{K}^+ \subset 2.2.2$ ) appears to act as a catalyst. These results, which concern the reaction of *p*-nitrophenyl methanesulfonate (1) with alkali-metal ethoxides, are reported here and are contrasted to results for other methanesulfonate

esters, including the *p*-trifluoromethylphenyl ester (2).



### Results

Kinetic data for the reaction of *p*-nitrophenyl methanesulfonate (1) with various alkali-metal ethoxide species are shown in Figure 1 and Table I. The observed rate constants increase in the order  $\text{LiOEt} < \text{NaOEt} < \text{CsOEt} \approx \text{KOEt} \approx \text{KOEt} + 18\text{C6} < \text{KOEt} + 2.2.2$ . A striking result in this system is the fact that potassium ethoxide in the presence of excess 2.2.2 cryptand is more reactive than either potassium ethoxide alone or potassium ethoxide in the presence of excess 18-crown-6 (Figure 1). If the data for  $\text{KOEt} + 18\text{C6}$  are taken to represent free ethoxide ion, as will be argued below, it follows that the potassium cryptate catalyzes the reaction which is inhibited by some uncomplexed alkali-metal ions ( $\text{Li}^+$ ,  $\text{Na}^+$ ) and relatively unaffected by others ( $\text{K}^+$ ,  $\text{Cs}^+$ ).

As seen in Figure 1, the plot of  $k_{\text{obs}}$  vs  $[\text{MOEt}]_0$  for  $\text{KOEt} + 2.2.2$  shows marked upward curvature, while plots for other ethoxide species are only slightly curved. In our previous treatment of ester ethanolysis reactions, curvature in plots of  $k_{\text{obs}}$  vs  $[\text{MOEt}]_0$

(1) (a) Bunzel, E.; Dunn, E. J.; Bannard, R. A. B.; Purdon, J. G. *J. Chem. Soc., Chem. Commun.* 1984, 162. (b) Dunn, E. J.; Bunzel, E. *Can. J. Chem.* 1989, 67, 1440. (c) Bunzel, E.; Pregel, M. J. *J. Chem. Soc., Chem. Commun.* 1989, 1566. (d) Dunn, E. J.; Moir, R. Y.; Bunzel, E.; Purdon, J. G.; Bannard, R. A. B. *Can. J. Chem.* 1990, 68, 1837. (e) Pregel, M. J.; Dunn, E. J.; Bunzel, E. *Can. J. Chem.* 1990, 68, 1846. (f) Pregel, M. J.; Bunzel, E. *J. Am. Chem. Soc.* 1991, 113, 3545. (g) Pregel, M. J.; Bunzel, E. *J. Chem. Soc., Perkin Trans. 2* 1991, 307. (h) Pregel, M. J.; Bunzel, E. *J. Org. Chem.* 1991, 56, 5583.